

Evolutionary approach for finding the atomic structure of steps on stable crystal surfaces

Ryan M. Briggs^{†,‡} and Cristian V. Ciobanu^{†, *}

[†]*Division of Engineering, Colorado School of Mines, Golden, Colorado 80401*

[‡]*Division of Engineering and Applied Science, California Institute of Technology, Pasadena, California 91125*

The problem addressed here can be concisely formulated as follows: given a stable surface orientation with a known reconstruction and given a direction in the plane of this surface, find the atomic structure of the steps oriented along that direction. We report a robust and generally applicable variable-number genetic algorithm for step structure determination and exemplify it by determining the structure of monatomic steps on Si(114)- 2×1 . We show how the location of the step edge with respect to the terrace reconstructions, the step width (number of atoms), and the positions of the atoms in the step region can all be simultaneously determined.

One-dimensional (1-D) nanostructures presently show tremendous technological promise due to their novel and potentially useful properties. For example, gold chains on stepped silicon surfaces^{1,2} can have tunable conduction properties, rare earth nanowires and bismuth nanolines have unusual straightness and length³ and can thus be useful as nanoscale contacts on chips or as templates for the design of other novel structures. The structure of step edges on silicon surfaces is of key interest, for it can help trigger a step-flow growth mode⁴ useful for preparing high-quality wafers. Understanding the formation, properties, and potential applications of these intriguing 1-D nanostructures requires knowledge of the atomic positions of various possible adsorbate species, as well as of the location of the silicon atoms at the step edges.

The determination of the atomic configuration at crystal surfaces is a long-standing problem in surface science. With the invention and widespread use of the scanning tunnelling microscope (STM) our understanding of crystal surfaces (in particular of surface reconstructions) has progressed immensely. Nevertheless, since the STM acquires information about the local density of states and not about the atomic positions, one still needs to find structural models that correspond to the images acquired. The problem becomes more challenging in the case of one-dimensional nanostructures on semiconductor surfaces (steps, surface-supported nanowires, atomic or molecular chains), because the step and nanowire structures may not be readily inferred from STM images given the possibility of having either flat supporting surfaces or vicinal ones with single- or multiple-layer steps. Even for a given direction and step height, the number of possible structures is daunting and their identification is tedious because it currently relies on relaxing ad-hoc structures that may or (more often) may not end up corresponding to the experiments. As seen in the case of Au^{1,2} or Ga⁵ on Si surfaces, one needs to propose a large number of atomic models and then check if they have sufficiently

low formation energies in order to ultimately identify or predict them as the actual physical nanostructures.

Motivated by the need to find good candidates for one-dimensional structures on surfaces, we have set out to develop a global search procedure that creates and selects atomic models based on their formation energy. To fix ideas, we address here the problem of predicting the atomic structure of steps along a given direction on a stable surface with a known reconstruction. While we focus on the case of straight steps on high-index semiconductor surfaces, we point out that the evolutionary procedure with variable atom numbers described below is generally applicable for finding the structure of any surface-supported 1-D nanostructure, provided that suitable (i.e. fast and reasonably transferable) interatomic potentials are available.

The particular 1-D systems chosen for this study are steps on stable high-index semiconductor surfaces [e.g., Si(114), Si(5512), Si(113)],^{6,7,8} which have a fundamental importance in addition to the practical one alluded above. Due to the lack of a robust approach for proposing and sorting step models, the pioneering study⁹ of steps on Si(001) was followed by only a few reports of step structures on other semiconductor surfaces.^{10,11,12} Focusing on the case of steps on the Si(114)- 2×1 surface, experiments show that straight steps form along the $[\bar{1}10]$ and the $[22\bar{1}]$ directions,¹³ which are precisely the directions of spatial periodicity of the reconstructed Si(114) unit cell.⁶ For each of the two directions we can define two types of steps (up and down), and for each step type there are two relative positions of the reconstructed unit cells on the upper and lower terraces: one in which the unit cells on terraces are in registry (normal) and another in which they are offset (shifted). A crystallographic analysis of the Si(114) surface shows that out of the four possible terrace configurations for each step direction there can be only two that are topologically distinct. The configurations that we have to address are therefore four, denoted here by $[\bar{1}10]$ -down, $[\bar{1}10]$ -up, $[22\bar{1}]$ -normal, and $[22\bar{1}]$ -shifted. Fig. 1a illustrates the $[\bar{1}10]$ -down configuration, while the remaining ones are described in note 14.

The methodology that we choose for finding the step

*Corresponding author; Phone 303-384-2119; Fax 303-273-3602; Email: cciobanu@mines.edu

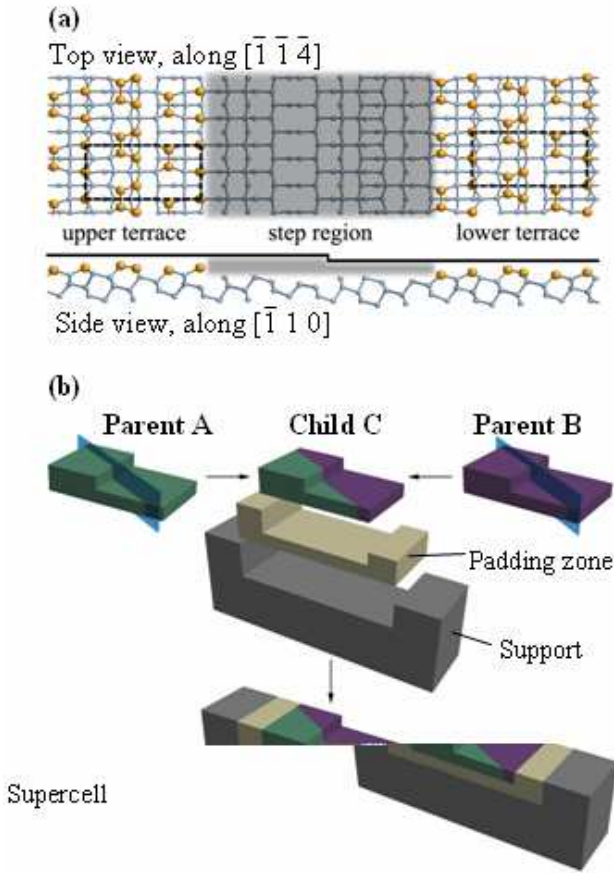


FIG. 1: (Color online)(a) Step region (shaded) for which the number of atoms, their positions, and the location of the step edge are to be determined. The step region, which corresponds to the $[\bar{1}10]$ -down configuration, is surrounded by reconstructed terraces with the surface unit cell marked by the dashed rectangles. (b) Crossover operation used in the genetic algorithm to search the configuration space. The step energy calculations involve relaxing a padding zone (in addition to the step region) with the supporting zone fixed.

structures is based on a genetic algorithm, which has been shown to achieve fast convergence using aggressive multi-particle moves for systems of any dimensionality from clusters to bulk crystalline materials (see, e.g., Refs. 15,16,17,18,19,20,21). In a rather simple but efficient way, the algorithm simulates a biological process in which a set of individuals evolves with the goal of producing fit children, i.e. new step structures with low formation energies. For all runs we have systematically kept a pool of $p = 30$ atomic structures and subsequently tested that a range of $30 \leq p < 100$ is appropriate for this problem, i.e. the pool is large enough that the evolution is not likely to get stuck in a local minimum and is sufficiently small so that the cross-over moves are not wasted optimizing mostly high-energy local minima. In general, the size of the pool should be determined by numerical experimentation for the particular system under study. The starting p structures (“Generation Zero”) are sim-

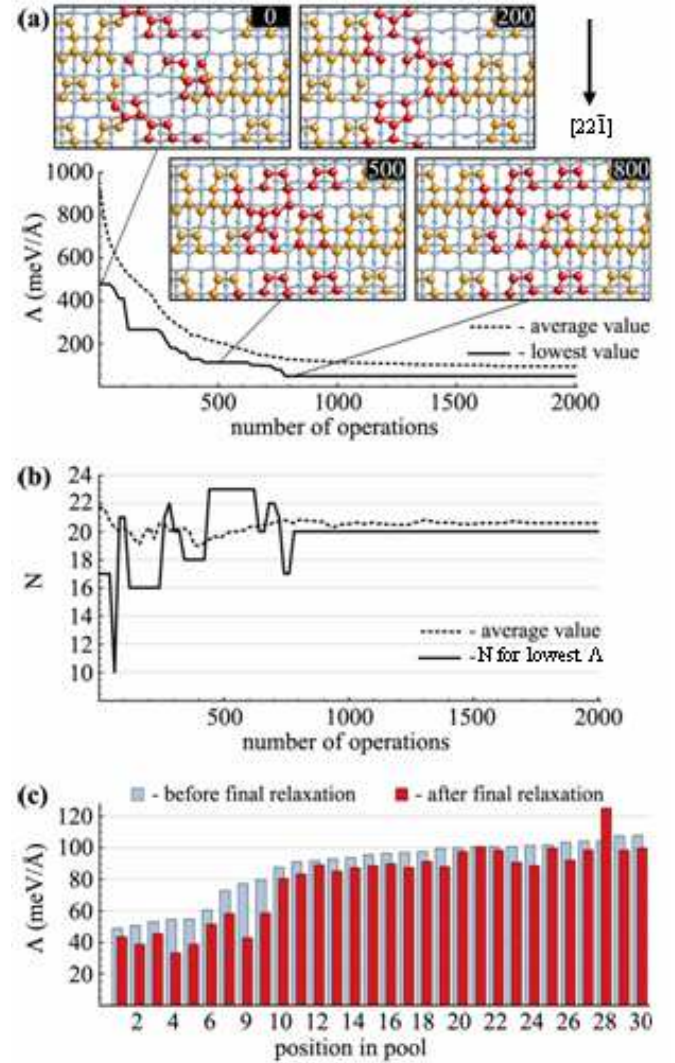


FIG. 2: (Color online) Finding the structure of $[2\bar{2}\bar{1}]$ -normal steps¹⁴ on Si(114). (a) Step energy Λ of the lowest-energy structure (solid line) and averaged across the pool (dashed line) during the genetic evolution. The lowest energy structure is shown after 0, 200, 500, and 800 crossover operations; the atoms subjected to optimization are shown as darker spheres in the insets. (b) Evolution of the average number of atoms across the pool (dashed line) and of the atom number corresponding to lowest-energy member (solid line). (c) Step energies before and after the final relaxation of all members of the genetic pool. The formation energies decrease upon full relaxation unless bonds are broken in the process (as found in the case of structure no. 28).

ply collections of atoms that are randomly positioned in the step region (colored gray in Fig. 1a) then relaxed to nearest local minima of the potential energy of the system. The evolution from the current generation to the next one occurs via crossover processes in which the step structures corresponding to two randomly chosen parents A and B from the pool are combined to create a new (child) structure, C . Referring to Fig. 1b, the crossover of parents A and B is achieved by sectioning them with

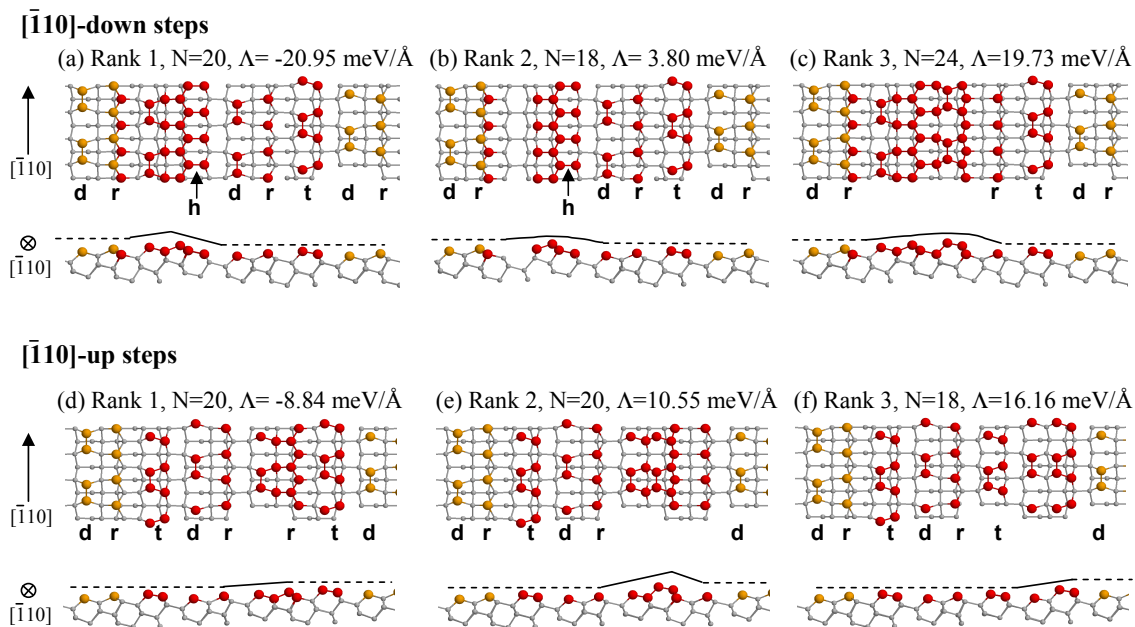


FIG. 3: (Color online) Low-energy step structures of $[\bar{1}10]$ -oriented steps on the Si(114) surface. The atoms subjected to optimization are represented by dark spheres, while the atoms making up the terrace reconstructions are the lighter ones. The remaining atoms are shown as smaller gray spheres. The structural motifs on the terraces are rows of dimers (d), rebonded atoms (r), and tetramers (t). Some or all of these motifs also make up the shown step structures with the exception of the most favorable down-step models [panels (a) and (b)] which include hexagon rows denoted by “h”. A schematic contour of the step topology was included in each side view to aid the eye.

the same random plane, then retaining atoms from each parent located on different sides of this plane to create the child C . The plane is chosen here to be parallel to $[114]$ (any polar angle about this direction is allowed) and located so as to pass through a randomly chosen point in the rectangle projected by the step zone onto the (114) plane. The operation so defined (Fig. 1b) has built-in potential to generate child structures with different numbers of atoms than their parents. Any child that is *structurally distinct from all pool members* is considered for inclusion in the genetic pool based on its formation energy per unit length, which should be lower than that of the highest ranked (i.e. least favorable) member of the pool. To preserve the total population, the structure with the highest formation energy is discarded upon inclusion of a new child. In a genetic algorithm run, the crossover operation is repeated to ensure that the lowest energy structure of the pool has stabilized; as such, the present systems require 2000 operations as illustrated by the curves in Fig. 2a which become flat as the algorithm progresses.

The formation energy of a step structure is defined as a per-length quantity that is in excess to the bulk and surface energies,²² and therefore can be written as

$$\Lambda = \frac{1}{L_y}(E_m - N_m e_b - \gamma A), \quad (1)$$

where E_m is the total energy of the N_m atoms that are allowed to move within a projected area $A = L_x L_y$ with

the dimension L_x (L_y) perpendicular (parallel) to the step, e_b is the bulk cohesion energy of Si, and γ is the surface energy of the flat Si(114) surface. The potential we have chosen to model the atomic interactions is the one developed by Lenosky et al.,²³ because it has shown reasonable transferability for diverse atomic environments present on high-index Si surfaces.^{18,20} If all the atoms of the supercell are allowed to move when calculating the formation energy [Eq. (1)], then each update of the genetic pool will be too slow for the algorithm to be practical. On the other hand, if we only relax the atoms in the step zone, then Eq. (1) will include not only the formation energy but also the elastic interactions of the step with the nearby rigid boundaries of the step region. To reach a good compromise between the full accuracy of Eq. (1) (which would be achieved when *all* atoms in the supercell are relaxed) and the speed required to sort out many structures per unit time, we introduce a padding zone that is relaxed along with the step region while the keeping the reconstructed support zone fixed (refer to Fig. 1b). The use of the padding zone will diminish the elastics interactions in Eq. (1) while keeping the number of atoms that are relaxed after each crossover small. At the end of any genetic algorithm run, a full relaxation (all atoms allowed to move) is performed for all pool members in order to refine the step energies.

Typical results of the genetic algorithm for steps are shown in Fig. 2a, which displays the evolution of the lowest and of the average formation energy of the genetic

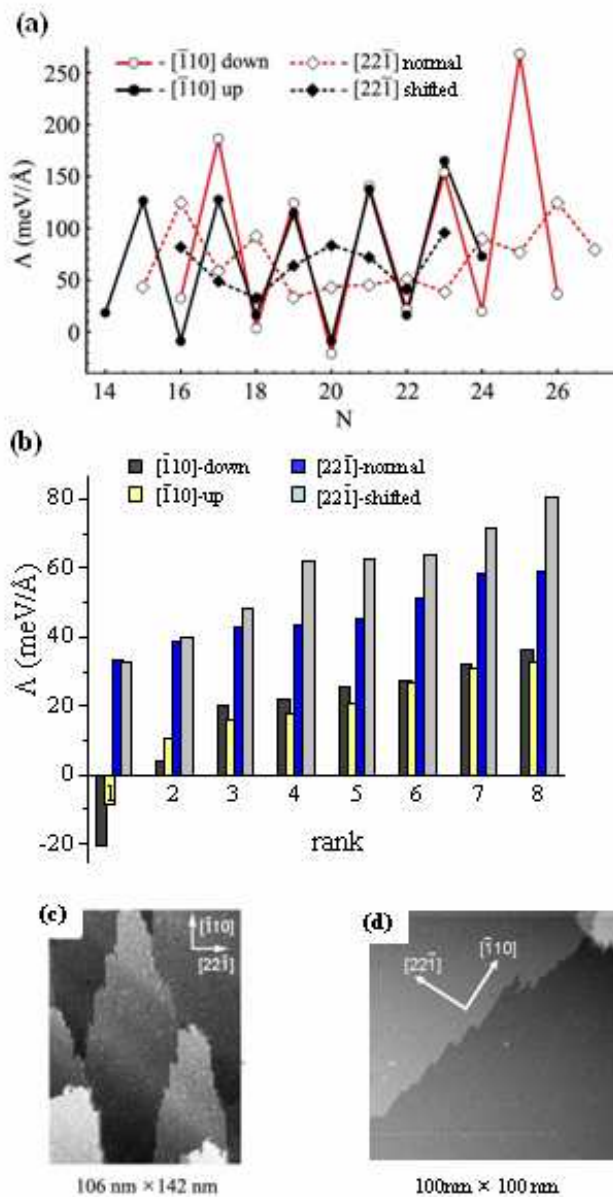


FIG. 4: (Color online) Results of the genetic algorithm (a,b) and experimental observations of steps on Si(114) surfaces (c,d). (a) Lowest step energies attained at various atom numbers in the step zone. (b) Final step formation energies of the top-ranking structures for each of the four types of steps described in text. The $[\bar{1}10]$ steps have consistently lower energies than similarly ranked $[22\bar{1}]$ structures. (c) STM image of a vicinal Si(114) surface obtained after cleaning and brief annealing (reproduced from Ref.13 with permission of the American Institute of Physics). (d) STM image taken after flashing at 1225°C followed by 30 minute annealing at 450°C (courtesy of D. E. Barlow, A. Laracuente, and L.J. Whitman). These experimental observations show that the $[\bar{1}10]$ steps are preferentially longer than the $[22\bar{1}]$ steps.

pool as a function of the number of crossover operations. Both the lowest and the average formation energies show a rapid decrease at the beginning of the evolution, followed by slower decay in the later stages. The lowest-energy $[22\bar{1}]$ -normal configuration was found in less than 1000 operations, and has been retrieved in four runs started from different Generation Zero scenarios with no significant change in the total number of crossover moves. Since the crossover operation described above creates new structures with variable numbers of atoms, the number of atoms N in the step region is optimized at the same time as the atomic positions (N is always smaller than the total number of atoms allowed to relax, N_m). Illustrative of the search for the optimal particle number N is Fig. 2b, which displays the evolution of the average number of atoms in the genetic pool and the particle number corresponding to the lowest-energy member. Fig. 2c shows that upon final full relaxation a certain amount of energetic reordering does occur, but this reordering is merely a refinement and does not eliminate from consideration any of the best structures deemed favorable prior to the complete relaxation of all step models in the pool. When using the algorithm for an arbitrary line defect, the formation energy comparison before and after final relaxation offers the most useful criterion for adjusting the size of the padding zone so as to provide sufficient relaxation without rendering the calculations intractable.

The best three structures for the up- and down-steps oriented along $[\bar{1}10]$ are shown in Fig. 3, along with their formation energies after the final relaxation and their optimal atom numbers N . The most favorable up-step and down-step both have negative formation energies, which is a known artifact of the empirical potentials.^{22,24} Without placing undue significance on the negative sign, we focus on the ranking of the formation energies and the corresponding structures. The reconstruction of the flat Si(114) surface consists of rows of dimers (d), rebonded atoms (r) and tetramers (t) in this specific periodic sequence (...-d-r-t-d-r-t-d-...) along the $[22\bar{1}]$ direction.⁶ Since we allowed for a large width of the step region,²⁵ the steps can negotiate their width and location during the genetic evolution. This is apparent in Fig. 3, which shows that the sequence of motifs (d, r, t) is continued seamlessly from each terrace into the step zone until the atomic structure and the location of the step edge are determined. The best $[\bar{1}10]$ down-step structures (Fig. 3a,b) include a row of hexagons (labelled by “h” in Fig. 3) in addition to motifs already encountered on the terraces. Other low-energy steps are observed to simply consist of a gap in the -d-r-t- sequence of the structural features on the terraces. For example, Fig. 3c shows a down step that contains dimers, rebonded atoms and tetramers in the correct order, but which are bonded to the upper (lower) terrace via elimination of one tetramer (dimer) row from the -d-r-t- sequence on the terraces. The most favorable up-step structures contain only rows of dimers and rebonded atoms (Fig. 3d), all motifs in a different or-

der (d-t-r, Fig. 3e), or only rows of dimers and tetramers (Figs. 3f). The algorithm is thus able to find narrow steps (Fig. 3d), wide ones (Fig. 3c), as well as steps with intermediate widths (Fig. 3a,b,e,f). This morphological and structural diversity is a tell-tale sign of the superior configuration sampling achieved here with just one simple genetic operation (the crossover, Fig. 1b).²⁶

To provide a closer look at the way the algorithm sorts through different numbers of atoms, we have plotted the lowest formation energy found for every number of atoms N attained *during* the evolution (Fig. 4a). Such a plot shows that the algorithm can visit, in the same evolution, several structures of particularly low formation energies (magic-number atomic configurations) and select them as part of the genetic pool. Magic structures are found for even values of N both for the up and down $[\bar{1}10]$ steps, as seen in Fig. 4a. The same figure shows that the formation energy of $[22\bar{1}]$ -normal steps also has a few distinct local minima, which are located at odd values of N . On the other hand, the $[22\bar{1}]$ -shifted configuration does not have magic number behavior. In this case, there are two deep minima for the range of atom numbers spanned, but after the final relaxation they are found to have the same structure only translated by one full terrace unit cell⁶ along the $[\bar{1}10]$ axis.

Finally, in Fig. 4b we report the formation energies of the lowest eight structures in the pool for each of the four configurations studied. The figure shows that the steps oriented in the $[\bar{1}10]$ direction have smaller formation energies than those along $[22\bar{1}]$ for all top ranking structures found. For the $[\bar{1}10]$ direction the down-steps are easier to form than the up-steps, while for the $[22\bar{1}]$ direction the up and down steps have identical structures and energies. The conclusion that $[\bar{1}10]$ steps are more favorable than $[22\bar{1}]$ steps is consistent with the general expectation that a direction of higher symmetry (i.e. $[\bar{1}10]$) yields lower step energies than a low symmetry one. Ideally, these results could be tested by recalculating the formation energy of steps at the level of density functional theory (DFT) calculations. While in principle DFT level calculations of formation energies of steps on Si(114) are tractable, the number of atoms involved is at least several hundred atoms which is beyond our present computational means.

However, we have found that existing experimental observations do support our genetic algorithm results, albeit qualitatively. Laracuate et al.¹³ reported STM images (reproduced here in Fig. 4c) in which the $[\bar{1}10]$ steps are clearly preferred over the $[22\bar{1}]$ ones even when, due to the preparation conditions¹³ steps may not assume the very lowest-energy structure for given direction and terrace configuration: this is consistent with the simulation results in Fig. 4b which show that $[\bar{1}10]$ steps are lower in energy for *metastable* structures ranked within the first eight at the end of the genetic evolution. More recently, Whitman and coworkers have also imaged step configurations after long anneals at 450°C. These recent measurements (shown in Fig. 4d) are more likely to corre-

spond to lowest-energy step structures, and again show that the $[\bar{1}10]$ are longer (more favorable) thus lending support to our simulation results. In terms of atomic positions, so far there has been no proposal for the structure of steps on Si(114). We have proposed here several low-energy structures (Fig. 3) found via the genetic procedure, structures which are amenable to experimental testing via high-resolution STM measurements combined with ab initio density functional calculations.

The versatile variable-number algorithm described in previous reports on two-dimensional surface systems^{18,20} has recently been extended to the case of 3-D crystal structure prediction.²¹ While in the 2-D and 3-D cases structure prediction methods were already available^{27,28} prior to the introduction of the genetic approaches,^{18,21} to our knowledge the present variable-number genetic algorithm is the first robust approach to atomic structure determination for surface-supported 1-D systems. A reader may rightfully argue that the use of empirical potentials could cast doubts on the results obtained by using this algorithm. Although empirical (or even tight-binding) potentials do have artifacts which lead to spurious minima, these minima may be accommodated to some extent by increasing the size of the pool. What makes the algorithm robust is not the specific potential model, but rather the concept of an evolved database whose optimized members (with different atom numbers and different structures) can be studied subsequently at any level of theory, including ab initio calculations. It is worth noting that, in fact, the reliance on empirical potential is much smaller in the present genetic algorithm than in the case of molecular dynamics and continuous-space Monte Carlo,^{27,28} because in the current implementation the genetic algorithm only relies on an acceptable accuracy of the local minima energies without the additional requirement of a good description of the height of the barriers between these minima.

In conclusion, we have presented a general way to determine the structure of steps on reconstructed crystal surfaces, and applied it to find the structure of monatomic steps on Si(114)- 2×1 . A key finding of this paper is that the step structure problem can be solved by what is probably the simplest genetic algorithm, i.e. an algorithm which is based on greedy selection of new members structurally distinct from the old ones and on a single real-space operation (cross-over between two parents using planar cuts). We speculate that the reason for which this simple approach works is that the underlying bulk crystal provides a strong template onto which the structure can relax while also obeying the periodic boundary conditions imposed. The bulk template lowers the number of both the distinct and the symmetry-equivalent configurations that the pool members can visit, and thus decreases the complexity of the problem as compared, e.g., with the optimization of an atomic cluster with the same range for the number of atoms. The variable-number approach is particularly well-suited for other problems beyond that of single-height steps on

clean high-index Si surfaces. Structure of the edge between two stable facets that bound a quantum dot, gold atom decorations of stepped surfaces,^{1,2,29} adsorbate-induced surface reconstructions,³⁰ steps on compound semiconductor surfaces,¹¹ and structure of step bunches during growth (e.g. Refs. 10,31) – to give a few significant examples – can be studied systematically using the procedure presented here, with the only necessary modifications concerning the geometry of the supercell and

the expression of the formation energy to account for a second atomic species.

Acknowledgment. CVC thanks Lloyd Whitman of the Naval Research Laboratory for very useful discussions and for graciously providing recent STM images of steps on Si(114) surfaces. We gratefully acknowledge the support of the National Center for Supercomputing Applications at Urbana-Champaign through grant no. DMR-050031.

-
- ¹ S. Riikonen and D. Sanchez-Portal, *Nanotechnology* **16**, S218 (2005).
- ² J.N. Crain, J.L. McChesney, F. Zheng, M.C. Gallagher, P.C. Snijders, M. Bissen, C. Gundelach, S.C. Erwin, and F.J. Himpsel, *Phys. Rev. B* **69**, 125401 (2004).
- ³ J.H.G. Owen, K. Miki, and D.R. Bowler, *J. Mat. Sci.* **41**, 4568 (2006).
- ⁴ W.K. Burton, N. Cabrera, and F. Frank, *Proc. Trans. Roy. Soc.* **243**, 299 (1951).
- ⁵ C. Gonzalez, P.C. Snijders, J. Ortega, R. Perez, F. Flores, S. Rogge, and H.H. Weitering, *Phys. Rev. Lett.* **93**, 126106 (2004).
- ⁶ S.C. Erwin, A.A. Baski, and L.J. Whitman, *Phys. Rev. Lett.* **77**, 687 (1996).
- ⁷ A.A. Baski, S.C. Erwin, and L.J. Whitman, *Science* **269**, 1556 (1995).
- ⁸ J. Dabrowski, H.J. Mussig, and G. Wolff, *Phys. Rev. Lett.* **73**, 1660 (1994).
- ⁹ D.J. Chadi, *Phys. Rev. Lett.* **59**, 1691 (1987).
- ¹⁰ S. Cereda, F. Montalenti, and L. Miglio, *Surf. Sci.* **591**, 23 (2005).
- ¹¹ Y. Temko, L. Geelhaar, T. Suzuki, and K. Jacobi, *Surf. Sci.* **513**, 328 (2002).
- ¹² S.B. Zhang and A. Zunger, *Phys. Rev. B* **53**, 127 (1996).
- ¹³ A. Laracunte, S.C. Erwin, and L.J. Whitman, *Appl. Phys. Lett.* **74**, 1397 (1999).
- ¹⁴ The reconstructed unit cell on terraces has dimensions of $3a \times a\sqrt{2}$, where $a = 5.431\text{\AA}$ is the bulk lattice constant of Si. The height of monatomic steps on Si(114) is $h = \sqrt{2}a/12$. The down and up $\overline{[110]}$ steps create intrinsic step-widths $\Delta = -11a/6$ and $\Delta = -7a/6$, respectively. In order to apply the non-orthogonal periodic boundary conditions²², the terrace must be lowered by an amount equal to h and translated along the step by $s_{\parallel} = \sqrt{2}a/4$ upon horizontal periodic displacements of length L_x . The supercell dimensions corresponding to the $\overline{[110]}$ steps are $L_x = 3ak + \Delta$ and $L_y = \sqrt{2}a$, where k is an integer set to be large enough ($k = 12$) that the elastic repulsion between the periodic images of the step is negligible. Steps in the $[2\overline{2}1]$ direction can differ only through the relative positioning of the reconstruction pattern on the upper and lower terraces. We found two such relative positions denoted as *normal* (for which $\Delta = -\sqrt{2}a/4$) and *shifted* ($\Delta = -3\sqrt{2}a/4$). The translation along the step direction for both of them is $s_{\parallel} = 7a/6$, and the dimensions of the supercell are $L_x = k\sqrt{2}a + \Delta$ and $L_y = 3a$.
- ¹⁵ D.M. Deaven and K.M. Ho, *Phys. Rev. Lett.* **75**, 288 (1995).
- ¹⁶ K.M. Ho, A.A. Shvartsburg, B.C. Pan, Z.Y. Lu, C.Z. Wang, J. Wacker, J.L. Fye, M.F. Jarrold, *Nature* **392**, 582 (1998).
- ¹⁷ B.L. Wang, S.Y. Yin, G.H. Wang, A. Buldum, J.J. Zhao, *Phys. Rev. Lett.* **86**, 2046 (2001); T.L. Chan, C.V. Ciobanu, F.C. Chuang, N. Lu, C.Z. Wang, and K.M. Ho, *Nano Lett.* **6**, 277 (2006).
- ¹⁸ F.C. Chuang, C.V. Ciobanu, V.B. Shenoy, C.Z. Wang, and K.M. Ho, *Surf. Sci.* **573**, L375 (2004).
- ¹⁹ H.J.W. Zandvliet, *Surf. Sci.* **577**, 93 (2005).
- ²⁰ F.C. Chuang, C.V. Ciobanu, C. Predescu, C.Z. Wang, and K.M. Ho, *Surf. Sci.* **578**, 183 (2005).
- ²¹ N.L. Abraham and M.I.J. Probert, *Phys. Rev. B* **73**, 224104 (2006). In the 3-D case, the authors showed that the variable-n genetic algorithm works with periodic cuts gives somewhat faster convergence (approx. 50% fewer moves) when compared with an algorithm that uses planar cuts.
- ²² T.W. Poon, S. Yip, P.S. Ho, and F.F. Abraham, *Phys. Rev. B* **45**, 3521 (1992).
- ²³ T.J. Lenosky, B. Sadigh, E. Alonso, V. V. Bulatov, T. Diaz de la Rubia, J. Kim, A. F. Voter, and J. D. Kress, *Modell. Simul. Mater. Sci. Eng.* **8**, 825 (2000).
- ²⁴ H.J.W. Zandvliet, *Rev. Mod. Phys.* **72**, 593 (2000).
- ²⁵ The size of the step zone was chosen so as to cover one full reconstructed unit cell on each side of the (initially arbitrary) step location.
- ²⁶ In most genetic algorithm implementations, mutations (small random displacements of arbitrarily selected atoms) are necessary to provide paths for the pool members to evolve towards global minima or towards stationary states³². Due to the requirement to allow only structurally distinct pool members at all times, mutations turned out to be unnecessary in the present algorithm.
- ²⁷ C.V. Ciobanu and C. Predescu, *Phys. Rev. B* **70**, 085321 (2004).
- ²⁸ M. Parrinello and A. Rahman, *J. Appl. Phys.* **52**, 7182 (1981); R. Martonak, A. Laio, M. Parrinello, *Phys. Rev. Lett.* **90**, 075503 (2003).
- ²⁹ S.K. Ghose, I.K. Robinson, P.A. Bennett, and F.J. Himpsel, *Surf. Sci.* **581**, 199 (2005).
- ³⁰ S.C. Erwin, *Phys. Rev. Lett.* **91**, 206101 (2003); H.S. Yoon, J.E. Lee, S.J. Park, and I.W. Lyo, *Phys. Rev. B* **72**, 155443 (2005); J.L. McChesney, J.N. Crain, F.J. Himpsel, and R. Bennewitz, *Phys. Rev. B* **72**, 035446 (2005); S. Riikonen, D. Sanchez-Portal, *Phys. Rev. B* **71**, 235423 (2005).
- ³¹ K. Sudoh, H. Iwasaki, and E.D. Williams, *Surf. Sci.* **452**, L287 (2000); F. Montalenti, P. Raiteri, D. B. Migas, H. von Kanel, A. Rastelli, C. Manzano, G. Costantini, U. Denker, O. G. Schmidt, K. Kern, and L. Miglio, *Phys. Rev. Lett.* **93**, 216102 (2004).

³² D.E. Goldberg, Genetic Algorithms in Search, Optimization and Machine Learning, Kluwer Academic Publishers,

Boston, MA (1989).